Viser Technology Pte. Ltd.
Research and Application of Materials Science
DOI: 10.33142/rams.v3i1.4497

Research Article Open Access

Gradient Ultra-fine Grained Surface Layer in 6063 Aluminum Alloy Obtained by Means of Rotational Accelerated Shot Peening

Ying LIU[1*], Hailu XU[2], He XIAN[1], Yanfang LIU[1], Zheng LI[1]*

1. School of Materials Science and Engineering, Nanjing University of Science and Technology, Nanjing 210094, China,
2. Faculty of Electrical and Mechanica, Pujiang College of Nanjing University of Technology, Nanjing 21100, China

***Corresponding authors:** Ying LIU, Zheng LI, Email: liuying517@njust.edu.cn; lizhengnust@foxmail.com*

Abstract:
Gradient ultra-fine grained surface layer in 6063 aluminum alloy was obtained by means of a novel surface self-nanocrystallization technique, namely rotational accelerated shot peening (RASP) treatment. The average grain sizes along the vertical section vary from hundreds of nanometers in the top surface to micrometers in the matrix. By using orthogonal experimental design to compare roughness values and hardness values, we synthesized the processing parameters to obtain sample of smaller roughness values and higher hardness.

Keywords: *rotational accelerated shot peening; gradient ultra-fine grained structure; orthogonal experimental design; processing parameters*

1 Introduction

The major failure modes of metallic engineering materials are fracture, corrosion and wear, which occurred or originated from the surface of materials. Therefore, it is significant to change surface micro-structures and compositions via physical and chemical techniques to satisfy the industrial requirements for the surface propertie [1].

In 1999, Lu K [2] combined the thought of the nano-structure with metal materials, put forward the surface nanocrystallization (SNC) concept, which through a certain physical or chemical methods, preparation of a surface layer with nano-grains of metal materials. At present, according to the function object classification, the surface nanocrystallization has three basic ways [3]: nanocrystallization by surface coating (or deposition); surface self-nanocrystallization; hybrid surface nanocrystallization. Self-nanocrystallization has mounts of methods, which mainly produce severe plastic deformation and promote grain refinement to the nanometer scale on the surface of the material under the action of external load repeatedly, including Ultrasonic Mechanical Vibration Technology, Supersonic Fine Particles Bombarding (SFPB) [4], Surface Mechanical Attrition Treatment (SMAT), Surface Rolling, Laser Shot Peening, etc. However, certain defects exist in some of these devices. Such as surface mechanical attrition treatment, it depends on vibrator to accelerate projectiles to impact on the surface. However, the projectile's velocity obtained is limited, which makes plastic deformation on the surface insufficient. Meanwhile, geometric shape of workable sample is relatively narrow and simple. Supersonic particle bombardment technology equipment is complex and expensive. The gun, carried the airflow and particle, is core components of super sound speed device. The strict design and material requirements and existence of unstable speed situation makes the technical equipment exist a certain distance from industrial production.

In view of the existing surface nano-technologies having many problems such as complex devices structure, small processing area and long processing time, etc, this paper proposes a new surface self-nanocrystallization devices, namely the Rotational Accelerated Shot Peening (RASP) surface treatment equipment. The technology uses turbine to accelerate projectiles to impact on the surface with a certain speed continuously, which produces strong plastic deformation in the surface to reach the purpose of grain refinement. This method is simple, safe and reliable with low cost of materials and equipment.

Mechanical properties of metallic materials improve after surface self-nano crystallization, such as strength,

Received on March 20, 2021; Accepted on April 23, 2021

hardness, wear resistance and corrosion resistance [5]. In this paper, by using RASP technique, gradient ultra-fine grained surface layer with a certain thickness was prepared for 6063 aluminum alloy. Moreover, optimum production technology parameters were obtained by changing the process parameters and orthogonal testing designation. The microstructure evolutions of the deformed surface layers were performed by TEM and other testing technology. The mechanical properties of samples were analyzed by means of portable roughness tester and hardness testing device.

2 Materials and Method

2.1 Experimental raw material

The experiment was performed on the 6063 aluminum alloy. The chemical composition is listed in table 1. Before processing, the sample surface use metallo graphic sandpaper for grinding to flat, and clean the surface with acetone and alcohol. Figure 1 is a metallographic image of original structure of 6063 aluminum alloy. as you can see from the picture, the grain boundaries of original sample are obvious, and distribution of grain size is uniform. The average size is about hundreds of micrometers, which means the original structure belongs to coarse grain structure.

Table 1 Chemical Composition of 6063 aluminum alloy (unit: wt%)

Component	Si	Fe	Cu	Mn	Mg	Cr	Zn	Ti	Ni	Al
Content	0.38	0.17	0.02	0.01	0.70	0.01	0.01	0.02	0.01	Allowance

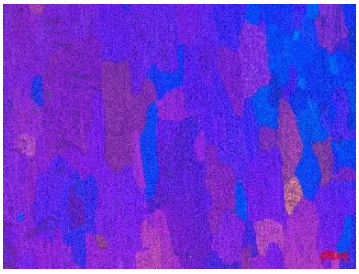

Figure 1 A metallographic image of original structure of 6063 aluminum alloy

2.2 Experimental installation

In this paper, the experimental installation is researched and developed by the research group of teachers and nanjing suinuo nano science and technology co., LTD., called Rotational Accelerated Shot Peening. RASP experiment is a method of self-nanocrystallization/ultrafine crystallization. The experiment equipment includes a workpiece room, steel projectile conveying system, shot peening host. Experimental schematic diagram is shown in Figure 2 The workpiece room: the sample in the workpiece chamber is fixed with clamping system. Clamping system can adjust the angle of the workpiece deflection institution to make the repeated impact more uniform. Steel projectile conveying system: using conveyor rubber belt, the system transmits projectiles to shot peening system; Shot peening system: the motor is used to drive the rotation of the impeller, blades of which accelerate projectiles to impact on the metal surface with a high speed under the action of centrifugal force. Severe plastic deformation occurs on the surface, finally leading to grain refinement. Velocity of projectiles depends on the speed of motor. The inferent energy can be controlled through changing the speed of motor, diameter of projectiles and processing time.

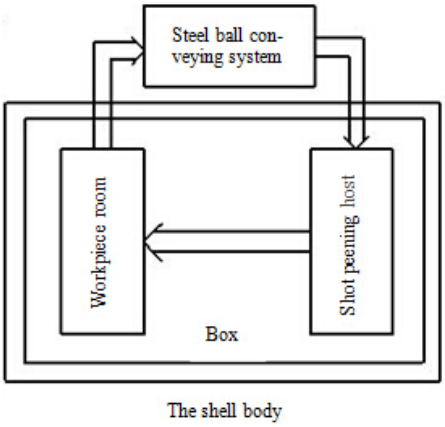

Figure 2 Experimental schematic RASP diagram (include the workpiece room, steel projectile conveying system, shot peening host)

Compared with the existing technology, rotational accelerated shot peening equipment has its significant advantages: (1) Simple structure. The design does not contain complex components, such as vibration device, which only consists of general motors and circulatory system. It is simple and compact structure, and convenient in installation, debugging and maintenance of the equipment. (2) High processing efficiency. This method make projectiles get kinetic energy by using the centrifugal acceleration device, so as to continuously hit the metal plate. The circulation system of the apparatus can convey a plurality of projectiles and it can be reused, which results in multiple bombardment on the surface in a unit of time and reducing the processing time. Compared with the above-mentioned methods of the surface nano-crystallization, the device increases single work area, reduces processing time, and improves work efficiency. (3) A wide range of samples' dimension. The equipment for processing multiple shaped materials, such as flat, circular arc shape or complex interface and other artifacts. This device can also process a variety of component materials, such as pure copper and 6063 aluminum alloy, steel hull, X80 pipeline steel, alloy steel, stainless steel, etc.

2.3 Experimental method

The specimens were processed by the RASP equipment. In order to find the optimal processing parameters with which the better properties can be obtained, in this paper, we make several groups of experiments with the orthogonal experimental design, and discuss the effect of parameters on the numerical results.

Orthogonal experimental design is a method of using orthogonal table to arrange and analyze multiple factors experiment. In all level combination of test factors, we select some represenative horizontal combination to experiment, then comprehensively understand test situation through this part of the test results, finally find out the optimal combinations of levels [6].

The experimental design index are roughness and hardness. The roughness value is as small as possible, while the higher the hardness is, the better it will be. There are three factors: the projectile's diameter, the velocity of projectile and processing time, without the interaction among various factors. Each level of influence factors are unequal, 2, 3 and 4, respectively, so we use mixed orthogonal table $L_{24}(2^{13}\times3\times4)$, orthogonal header design as shown in table 2.

The projectile materials of the experiment is high precision rolling bearing steel GCr15. the specific processing parameters are the projectile's diameter (unit: mm), the velocity of projectiles (m/s) and processing time (min). A total of experiments are 24 groups. All experimental parameters are shown in table 2. These parameters are all a factor regarded as a variable, two other factors remaining unchanged, to reflect the relationship between them.

3 Experimental results and analysis

The roughness of deformed coarse grained aluminum was measured by a portable surface roughness tester RTP-220. The micro-hardness was tested by HMV-G21 micro-hardness tester, using static indentation method. Measuring hardness variation along the depth direction,the load is 98.07mN, the loading time is 10 s. TEM samples were prepared by mechanical grinding, then ion thinning. Tecnai G220 S-TWIN transmission electron microscope (six lanthanum boride) was used to analyze microstructure of samples after treatment.

3.1 Roughness and Hardness

The roughness and hardness is analyzed by using the method of orthogonal experiment to discuss the results in 24 groups of experiments. To analyze the experimental results, It is necessary to calculate the value of K (K is sum of the same level), k value (The average value of each factor of the same level) and range value R [6]. According to the k values, we can

Table 2 Table of orthogonal test designing (three factors without interaction and the corresponding level)

The experimental parameters	
3mm,10m/s,5min	5mm,10m/s,5min
3mm,10m/s,15min	5mm,10m/s,15min
3mm,10m/s,30min	5mm,10m/s,30min
3mm,10m/s,60min	5mm,10m/s,60min
3mm,15m/s,5min	5mm,15m/s,5min
3mm,15m/s,15min	5mm,15m/s,15min
3mm,15m/s,30min	5mm,15m/s,30min
3mm,15m/s,60min	5mm,15m/s,60min
3mm,25m/s,5min	5mm,25m/s,5min
3mm,25m/s,15min	5mm,25m/s,15min
3mm,25m/s,30min	5mm,25m/s,30min
3mm,25m/s,60min	5mm,25m/s,60min

Table 3 The experimental parameters(the projectile's diameter (unit: mm), the velocity of projectiles; (m/s) and processing time(min)

FactorsLevel No.	The projectile's diameter (mm)A	The projectile's velocity (m/s)B	Processing time (min)C
1	3	10	5
2	5	15	15
3		25	30
4			60

Table 4 Analysis and results (ascertain primary and secondary order, optimal levels, optimal combination)

	Experiment No.	Factors		
	1—24	A	B	C
Roughness	κ_1	200.4	174.6	229.6
	κ_2	205.6	125.9	264.1
	κ_3		309.8	164.9
	κ_4			154.4
	R	5.2	183.9	110.7
	Primary and secondary order		B＞C＞A	
	Optimal levels	A_1	B_2	C_4
	Optimal combination		$A_1B_2C_4$	
Hardness	k_1	67.2	66.6	68.2
	k_2	68.4	66.7	71.3
	k_3		71.03	61.6
	k_4			67.5
	R	1.2	7.3	9.7
	Primary and secondary order		C＞B＞A	
	Optimal levels	A_2	B_3	C_2
	Optimal combination		$A_2B_3C_2$	

determine the optimal level, and select the optimal combination. Primary and secondary order of factors are based on the value of R. The larger values of R is, the more influence on experimental index the change level of the factor has. indicates the factor more important. The analysis and results are shown in table 3.

In conclusion, the best process parameters tentatively are summarised as follows: a) the roughness: 3mm, 15m/s, 60min; b) the hardness: 5mm, 25m/s, 15min. Overall balance determine the optimal process conditions. According to the factors of primary and secondary, optimization of conditions of the above two indexes isolate inconsistencies must be comprehensive consideration to determine the optimum process conditions. For factor B, the excellent level is B_2 for the effect on roughness, which is the primary factor. While for the influence on hardness, the optimal level is B_3, which is the secondary factor for it. If the level B_2 is selected, the roughness is 172% lower than that in B_3. While the hardness value is similar, so level B_2 is choose as the optimal level. Factor C, it is the secondary factor for influence on the roughness, the primary factor for effect on the hardness. When the main consideration is roughness, the optimal level is C_4, on the contrary, the optimal level is C_2. If C_2 is selected, the roughness nearly two times higher than that in C_4, while the hardness value is similar. as a result, for factor C, the optimal level is C_4. The factor A, its effect on the roughness and hardness are not significant. In the condition of B_2 to be taken for factor and C_4 to be taken for factor C, the roughness in A_2 is 42% higher than that in A_1, while the hardness increase by 3%, so the optimal level is A_1 for factor A. To sum up, the best process parameters are shown as follows: 3mm, 15m/s, 60min.

3.1.1 The roughness results and analysis

Table 4 shows that for the roughness, the primary and secondary order of Impact factors is B＞C＞A, that is to say, B is the main factor, C is a minor factor, and A is unimportant factor. Figure 3 is a diagram of roughness. Figure 3 a) is a diagram of the projectile velocity regarded as a variable. The figure shows ceteris paribus, the surface roughness value is lager with projectile velocity increasing. When process parameters are 3mm, 10m/s, 5min, the surface roughness value reaches to minimum, about 96 μm. While parameters are 5mm, 25m/s, 60min, the surface roughness is minimal, about 424 μm. When the diameter of projectile is 3mm, projectile velocities are 10m/s, 15m/s, 25m/s respectively, the surface roughness of the samples was less than 200 μm, that is to say, the sample surface is neat, which is similar to the situation of projectile diameter 5mm, projectile velocity 10 m/s, 15 m/s. While projectile diameter is 5 mm, and projectile velocity is 25 m/s, the surface roughness increases obviously, namely, the sample surface is more uneven. Figure 3 b) is diagram of processing time regarded as a variables. From the figure, ceteris paribus, the sample surface is more uneven with increasing of processing time. When process parameters are 3 mm, 15 m/s, 60 min, the surface roughness value is about 160 μm, namely, the sample surface is relatively flat. When processing time sustains constant, the surface roughness of parameters for 5mm, 25m/s is far higher than the other parameters. The possible reason may be that as the experiment carried out, the projectile energy continues to increase, the surface deformation work increases, dynamic recovery occurs to soften it,

which means continuous impact on the sample surface will make its surface pits increasing, finally the surface roughness becomes higher. Figure 3 c) is a diagram of projectile diameter regarded as a variable. It can be seen from the figure that ceteris paribus, the surface roughness value is higher with projectile diameter increasing. When the process parameters are 25 m/s, 15min, the surface roughness of projectile diameter of 5 mm (200 μm) is almost double that of projectile diameter of 5 mm (120 μm). In the same situation, When the process parameters are 25 m/s, 60min, the surface roughness of projectile diameter of 5 mm (424 μm) is much higher than that of projectile diameter of 5 mm (200 μm), that is to say, smaller projectiles will lead to flat surface[7]. This phenomenon is similar to the electric spark line cutting relationship between energy and roughness, i.e., the surface roughness increases correspondingly with the cutting speed [8].

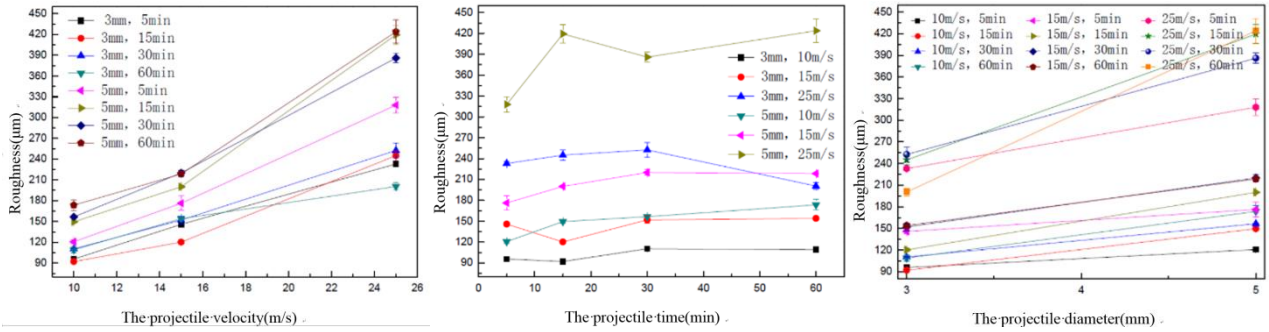

a) b) c)

Figure 3 Diagrams of roughness. a) projectile velocity regarded as a variable; b) projectile processing time regarded as a variable; c) projectile diameter regarded as a variable

3.1.2 The micro-hardness results and analysis

Table 4 shows that for the micro-hardness, the primary and secondary order of Impact factors is C＞B ＞A, that is to say, C is the main factor, B is a minor factor, and A is unimportant factor. Figure 4 is a diagram of micro-hardness. Figure 4 (a), (b) are diagrams of projectile velocity regarded as a variable. The figure shows ceteris paribus, the hardness values are lager with projectile velocity increasing. In figure 4 (c), processing time is treated as a variable. The figure shows when the projectile diameter is 5 mm, the micro-hardness of gradient structure increases and then decreases with processing time increasing, that is, there exists a critical value. When Processing time increases to 60 min, micro-hardness reduced, the reason of which may be temperature of the sample rises during RASP treating process, leading to dynamic recrystallization in the surface, then making grain growth occur [9].

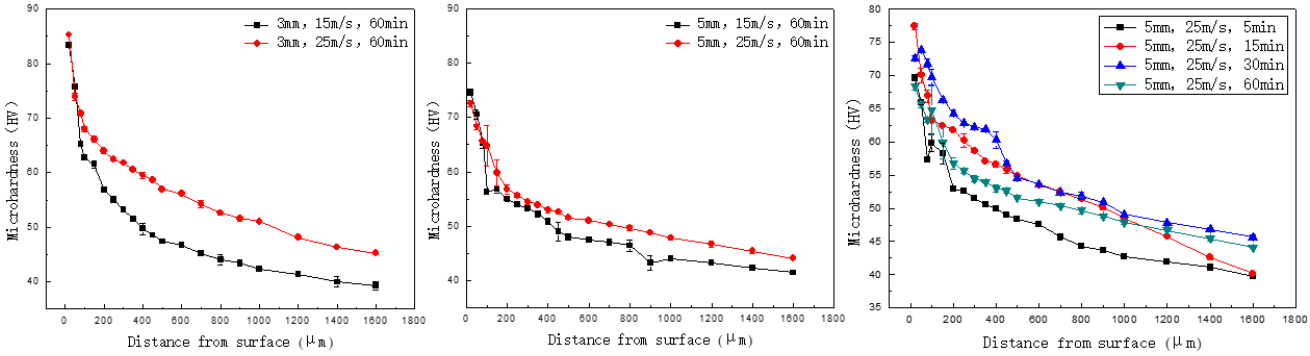

a) b) c)

Figure 4 Diagrams of hardness. a) projectile velocity regarded as a variable (3mm,15m/s, 25m/s, 60min); b) projectile velocity regarded as a variable (3mm, 15m/s, 25m/s,60min); c) processing time regarded a sa variable (3mm, 25m/s, 5min,15min, 30min, 60min)

Figure 5 are diagrams of projectile diameter regarded as a variable. The figure shows ceteris paribus, namely 15m/s, 60min, two kinds of topmost surface hardness are close. While the projectile velocity is 25m/s, and processing time is 60min, the sample surface hardness with the projectile diameter of 3 mm is larger than the diameter of 5mm. This is probably because recrystallization or grain growth may occur in the surface layer, resulting in lower hardness [10]. It requires subsequent experiments for further certification. Figure 4 and figure 5show that the micro-structure treated by RASP is gradient structure, namely, the hardness value decreases along the vertical section from surface to matrix. At the same time, the surface micro-hardness

increases significantly [11]. When the process parameters are 3mm/5mm, 15m/s, 60min, micro-hardness of two samples are similar, but we can see from Figure 3, the surface roughness value of former specimen is much smaller than the latter. When the process parameters are 5mm, 25m/s, 15min, 30min and 60min, the surface hardness of the former sample is much larger than the latter, the reason of which may be that as the experiment keep going, the deformation in the surface becomes more several, and dynamic recrystallization produced, leading to grain growth in the surface layer, which results in lower hardness, conforming to the Hall-Petch relationship [12]. Through the above analysis, the optimal process parameters are 3 mm, 15 m/s, 60min, which is consistent with the analysis of orthogonal experiment.

In summary, there is a critical value of the projectile energy. When the projectile energy is lower than this value, the upper the projectile energy is, the higher the hardness value is. Because under the action of external force, plastic deformation occur on the surface, which leads to dislocation slip, appreciation, tangle ,resulting in grain refinement in the surface layer, showing hardness decrease. Plastic deformation carries on, which is conducive to improve the hardness of the metal[13]. When the projectile energy is higher than this value, the upper the projectile energy is, the smaller the hardness value is. Because exorbitant energy causes dynamic recrystallization in the surface layer, resulting in grain growth and hardness decrease.

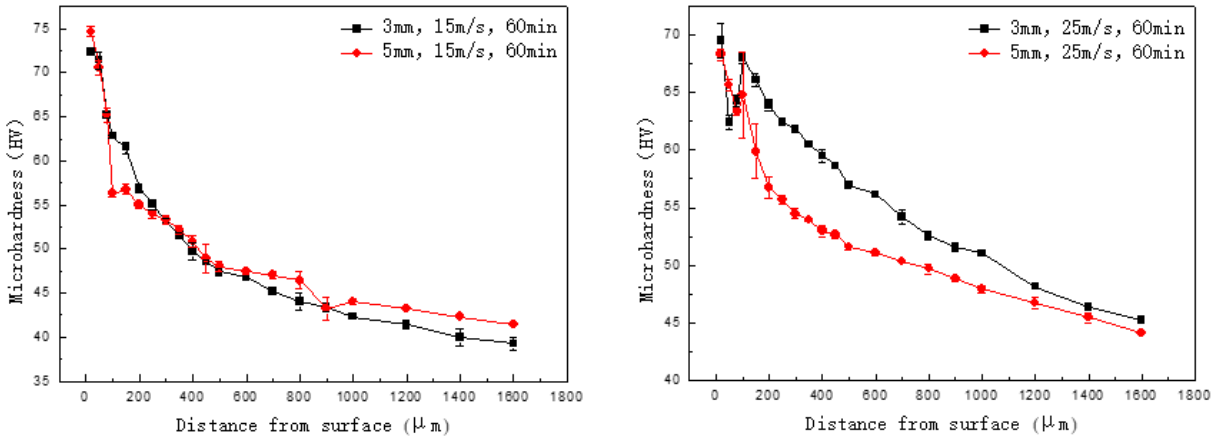

Figure 5 Diagrams of hardness with projectile diameter regarded as a variable. a) 3mm, 5mm, 15m/s, 60min; b) 3mm,5mm, 25m/s, 60min

3.2 TEM results and analysis

The microstructure of surface layer treated by RASP (plane sample: the topmost surface , splicing sample: vertical section) can be observed by using TEM experiment. According to images of morphology, the average grain size of vertical section along the topmost surface to the matrix can be kept statistics.

Figure 6 shows TEM bright field images of topmost surface in 6063 aluminum alloy treated by RASP treatment with different parameters. It is shown that after RASP treatment, grain refinement is obvious, grain orientation is random and the grain size of surface layer is respectively about 500 nm (a), 512 nm (b) and 528 nm (c), which means the microstructure is ultrafine structure.

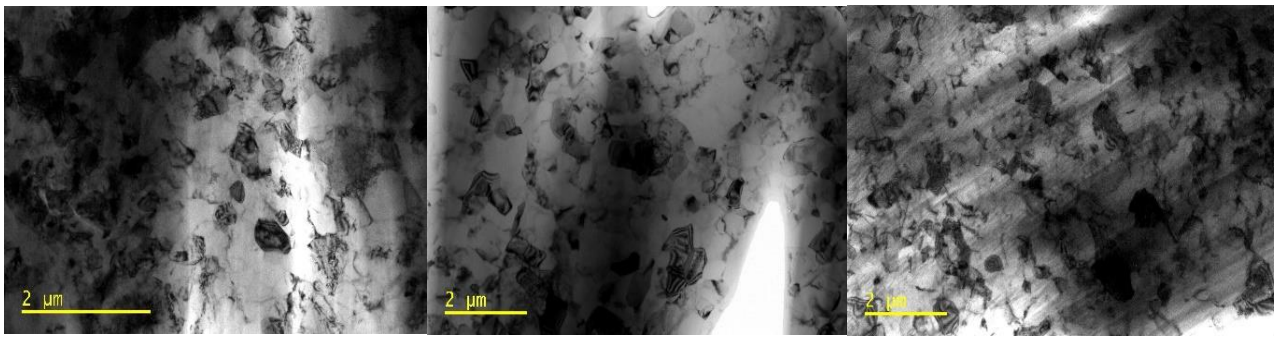

(a) 3mm、15m/s、60min (b) 3mm、25m/s、30min (c) 5mm、25m/s、30min

(the experimental parameters are 3mm,15m/s,60min; 3mm,25m/s,30min; 5mm,25m/s,30min, respectively)

Figure 6 TEM bright field images of topmost surface in 6063 aluminum alloy treated by RASP treatment.

Figure 7 shows TEM bright field images of gradient structure in 6063 aluminum alloy treated by RASP

treatment along vertical section from topmost surface to about 150 μm (3mm, 25m/s, 60min), 150 μm (5mm, 25m/s, 15min), 300 μm (5mm, 25m/s, 30min) depth. From the figures, we can see, after RASP treatment, grain refinement in the surface layer is obvious, and with the depth increasing from the surface, the grain size increases, showing obvious gradient structure. The figure 7 also shows the average grain size of different depth from topmost surface. Through the graph, after RASP processing, the surface layer realizes grain refinement, and experimental evidences show that after the RASP treatment the microstructure of the surface layer may be refined to the ultrafine-scale [14].

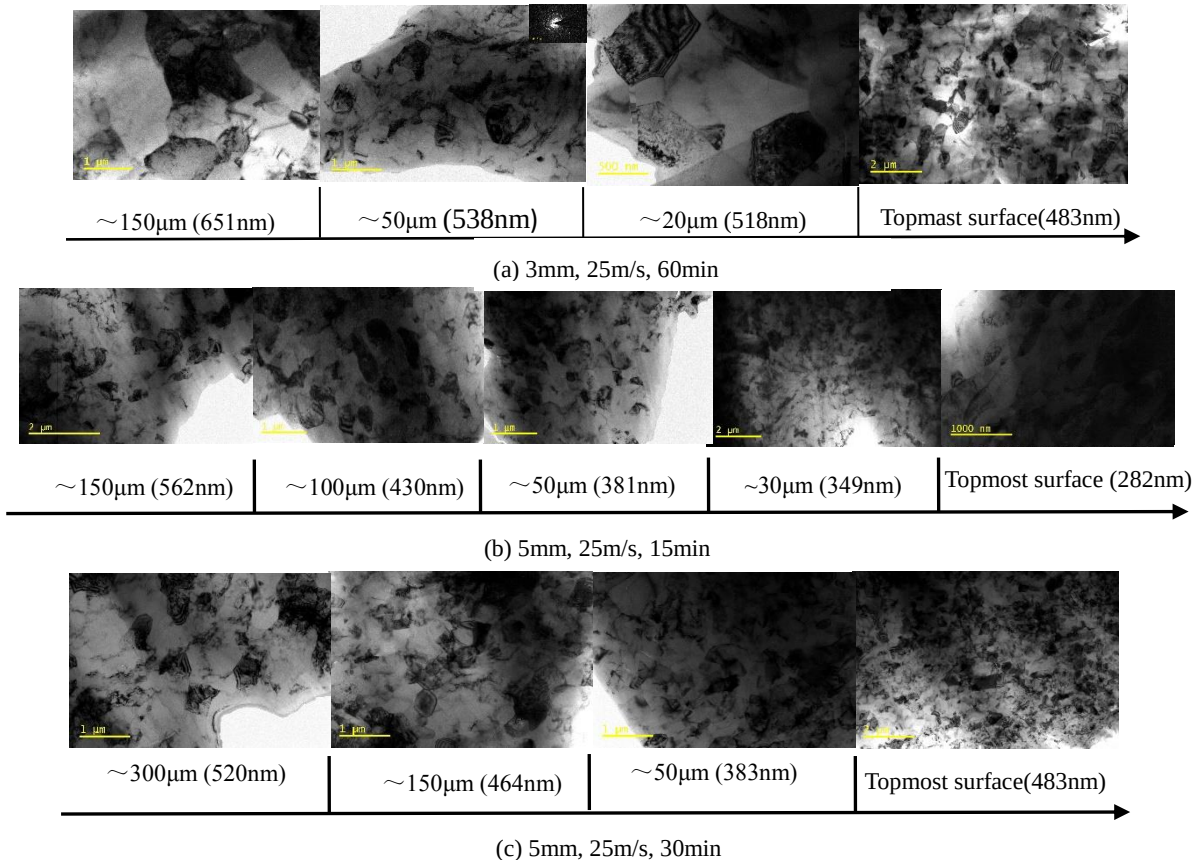

Figure 7 TEM bright field images of gradient structure in 6063 aluminum alloy treated by RASP treatment along vertical section from topmost surface to about 150 μm (3mm, 25m/s, 60min), 150 μm (5mm, 25m/s, 15min), 300 μm (5mm, 25m/s, 30min) depth

Figure 8 shows TEM bright field images of high-density dislocation walls (DDWs) and dislocation tangles (DTs) at the topmost surface in 6063 aluminum alloy treated by RASP treatment. With the increase of strain, there are more and more dislocations. These dislocations come together, forming high-density dislocation walls and dislocation tangles.

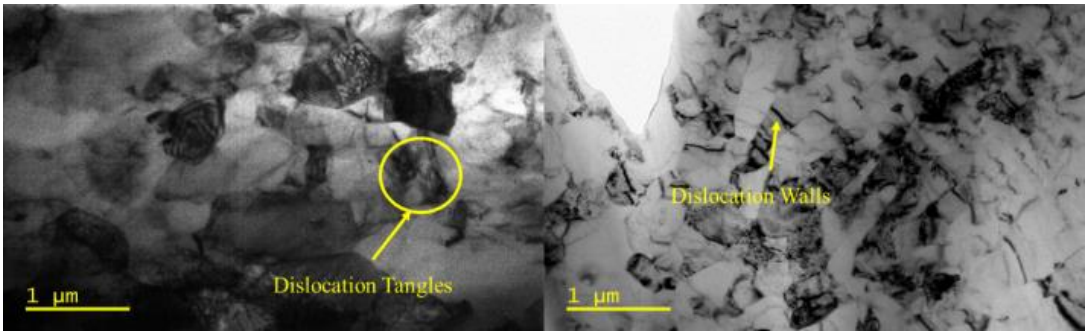

(a) 3mm, 25m/s, 60min (b) 5mm, 25m/s, 15min

Figure 8 TEM bright field images of high-density dislocation walls and dislocation tangles at the topmost surface

Figure 9 is average grain size of the topmost surface in 6063 aluminum alloy treated by RASP

treatment . The figure shows that the surface grain size of all the samples are less than 550 nm, which suggests RASP treatment technology achieves grain refinement to ultrafine-scale, and the process parameters for 5mm, 25m/s, 15min reach to the best refinement effect. From the graph, we also can conclude that, when the projectile diameter and velocity (5mm, 25m/s) are limited, the sample surface grain size is smaller with processing time decreasing. When the projectile diameter and processing time (3mm; 60min) are limited, the sample surface grain size decreases with projectile velocity increasing.

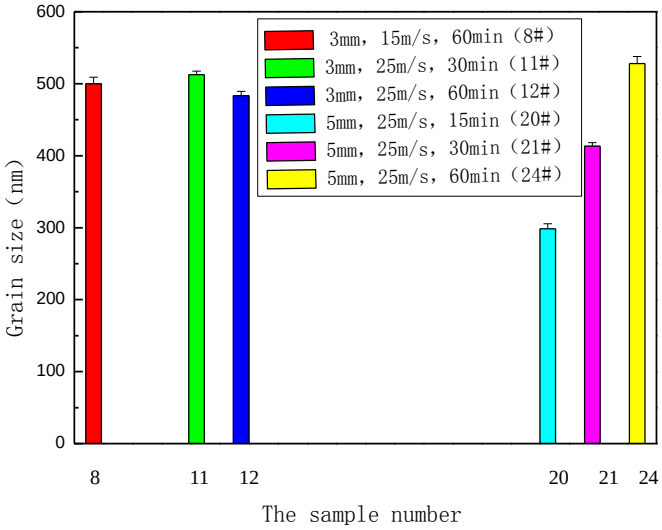

Figure 9 Average grain size of the topmost surface in 6063 aluminum alloy treated by RASP treatment

(the experimental parameters are 3mm,15m/s,60min; 3mm, 25m/s, 30min; 5mm, 3mm, 25m/s, 60min; 5mm,25m/s, 15min; 5mm, 25m/s, 30min; 5mm, 25m/s,60min, respectively)

The above analysis shows that plastic deformation occurs in the surface layer during RASP processing, producing a large number of dislocations, forming a high density of dislocations and dislocation tangles wall, which changes the grain boundary and then converts to large angle sub-grain boundary by constantly absorbing dislocations. Coarse grains refine to subgrains through the above process, which is repeated, achieving grain refinement. With the projectile energy (associated with the projectile diameter and speed) increasing, grain refinement increases then decreases. The reason of decrease may be it is easy for dislocations to be absorbed in higher temperature, which results in a dynamic recovery, decrease of density of dislocations, increase of grain boundary misorientation, leading to the large angle grain boundary percentage and the average misorientation increasing[15]. Therefore, for the metals with high stacking fault energy, dynamic recovery hinders the processing of grain refinement.

4 Conclusions

In this paper, using metallographic microscope, TEM and other testing technology analyzes the microstructure and microstructure change in 6063 aluminum alloy treated by RASP treatment and preliminary study of micro-mechanism of grain refinement. Portable roughness tester and hardness tester are used to measure the surface properties. The experimental conclusions are as follows:

(1) When projectile velocity regarded as a variable, the figure shows ceteris paribus, the surface roughness value and hardness is lager with projectile velocity increasing; Projectile diameter regarded as a variable, ceteris paribus, namely 15m/s, 60min, two kinds of topmost surface hardness are close. While the surface roughness value is higher with projectile diameter increasing; Processing time treated as a variable, when the parameters are 5 mm, 25m/s, the micro-hardness of gradient structure increases and then decreases with processing time increasing, that is, there exists a critical value.

(2) While the sample surface is more uneven with increasing of processing time. With all that said, the optimum process parameters is 3mm, 15m/s, 60min, which can achieve higher hardness and flatter surface.

(3) 6063 aluminum alloy is FCC structure with high stacking fault energy. Under the external loads, it has severe plastic deformation in the surface layer, which leads to dislocation movement, forming high-density dislocation walls (DDWs) and dislocation tangles (DTs). Through gradually absorbing dislocations, dislocation walls and dislocation tangles evolves to small angle sub-grain boundaries; small angle sub-grain boundaries continue to absorb dislocations to form large angle grain boundaries; The above process is repeated in sub-grain, leading to the grain size decrease, the misorientation increase, and finally equiaxed and randomly oriented

ultrafine grains are obtained. The surface hardness increase is mainly due to work hardening and grain refinement strengthening effect.

Acknowledgements: This research used the resources of the Nanjing University of Science and Technology analytical and testing center. This research was funded by NSFC (Grant No. 51301092) and the National Key R & D Program of China (Grant No. 2017YFA0204403). Open Research Fund of Science and Technology on High Strength Structural Materials Laboratory (No. O2016006).

References

[1] K LU, J LU. Nanostructured surface layer on metallic materials induced by surface mechanical attrition treatment[J]. Mater. Sci. Eng. A, 2004, 10(3):38-45.

[2] K LU, J LU. Surface Nanocrystallization (SNC) of Metallic Materials Presentation of the Concept behind a New Approach [J]. Mater. Sci. Technol,1999, 15(3):193-197.

[3] Liu G, Yong X P, Lu K. Surface nanocrystallization In Metal and Its Present [J]. China Surface Engineering, 2001, 52(3): 1-5

[4] Ba D M, Ma S N, Li C Q. Surface nanocrystallization Research In Supersonic Particles Bombard the Surface of 45 # steel[J]. Journal of materials science and technology, 2007, 15 (3): 342-342.

[5] F. J. Humphreys. A unified theory recovery, recrystallization and grain growth, based on the stability and growth of cellular microstructure. The base model [J]. Acta mater, 1997, 45(10): 4231-4240.

[6] L Liu, P Y Li. Orthogonal experiment and optimization of heat treatment process of the 34CrNi3Mo steel [J]. Material heat treatment technology, 2011, 1(6):164-166.

[7] K. Dai, J. Villegas, Z. Stone, L. Shaw. Finite element modeling of the surface roughness of 5052 Al alloy subjected to a surface severe plastic deformation process [J]. Acta Materialia, 2004, 52: 5771-5782.

[8] L Yang, A J Cai. Research on WEDM Process Parameters on the effects of the machining speed and surface roughness [J]. Machine tools and hydraulics, 2011, 39(15):45-47.

[9] H Liu. Research status of metal material surface nanocrystallization [J].Petroleum engineering construction, 2010, 36(3):11-15.

[10] G Y Qiao, Q P Sheng. The research status of metal surface self nanocrystallization by application of ultrasonic [J]. Oral material equipment, 2011, 20(2):101-105.

[11] J C Villegas, L L Shaw. Nanocrystalline process and mechaniism in a nickel alloy subjected to surface severe plastic deformation [J]. Acta Materialia, 2009,57: 5782-5795.

[12] Farahbakhsh I, Zakeria A, Manikandan P, Evaluation of Nanostructured coating layers formed on Ni projectiles during mechanical alloying of Cu powder [J]. Applied Surface Science, 2010, 358: 2354-2359.

[13] Romankov S, KomarovS V. Fabrication of TiN coatings using mechanical milling techniques [J]. Int. J. Refract. Met. HardMater, 2009, 27: 492-497.

[14] Xu C, Horita Z, Langdon T G. Microstructural Evolution in 6063 aluminum alloy uminum in the Early Stages of Processing by High-Pressure Torsion [J]. Materials transactions, 2010, 51(1): 2-7.

[15] K. Wang, N.R. Tao, et al. Plastic strain-induced grain refinement at the nanometer scale in copper [J]. Acta Materialia, 2006, 54: 5281-5291.